

Article

Fluid Retrofit for Existing Vapor Compression Refrigeration Systems and Heat Pumps: Evaluation of Different Models [†]

Dennis Roskosch ^{*}, Valerius Venzik and Burak Atakan 

Department of Mechanical and Process Engineering, University of Duisburg-Essen, Thermodynamics, Lotharstr. 1, 47057 Duisburg, Germany; valerius.venzik@uni-due.de (V.V.); burak.atakan@uni-due.de (B.A.)

^{*} Correspondence: dennis.roskosch@uni-due.de

[†] This paper is an extended version of our paper published in 2018 Heat Powered Cycles Conference, Bayreuth, Germany, 16–19 September 2018; ISBN 978-0-9563329-6-7.

Received: 25 April 2019; Accepted: 20 June 2019; Published: 24 June 2019



Abstract: The global warming potential of many working fluids used nowadays for vapor compression refrigeration systems and heat pumps is very high. Many of such fluids, which are used in currently operating refrigerators and heat pumps, will have to be replaced. In order to avoid a redesign of the system, it would be very helpful if efficient and ecological alternative working fluids for a given plant could be found. With modern process simulation tools such a selection procedure seems possible. However, it remains unclear how detailed such a model of a concrete plant design has to be to obtain a reliable working fluid ranking. A vapor compression heat pump test-rig is used as an example and simulated by thermodynamic models with different levels of complexity to investigate this question. Experimental results for numerous working fluids are compared with models of different complexity. Simple cycle calculations, as often used in the literature, lead to incorrect results regarding the efficiency and are not recommended to find replacement fluids for existing plants. Adding a compressor model improves the simulations significantly and leads to reliable fluid rankings but this is not sufficient to judge the adequacy of the heat exchanger sizes and whether a given cooling or heating task can be fulfilled with a certain fluid. With a model of highest complexity, including an extensive model for the heat exchangers, this question can also be answered.

Keywords: refrigerants; retrofit; process simulation; replacement fluids; experiments

1. Introduction

As a result of the Montreal Protocol [1], chlorofluorocarbons (CFCs), which previously were used as working fluids in compression refrigeration cycles and heat pumps, were replaced by substances without ozone depletion potential. Hydrofluorocarbons (HFCs), like R134a, R404A and, R410A, are good alternatives. They are still used in a wide range of systems today. Some HFCs, although they have no ozone depletion potential, have an extremely high global warming potential (GWP). They contribute significantly to global climate change. The United Nations (UN) therefore, decided to reduce their usage. The resolution of the UN is implemented in the European Union by the F-Gas-Regulation [2] and it includes several different instruments. Direct usage bans apply to refrigerants with a GWP greater than 2500 (e.g., R404A) and a filling capacity exceeding 40 t CO₂ equivalents (according to Reference [3]) in the next few years (2020 or 2022). Smaller plants such as those used as household air conditioning systems or heat pumps are affected by a phase-down scenario. This specifies that the quantity of newly produced synthetic refrigerants (measured in CO₂ equivalents) placed on the EU market will have to be reduced gradually with reference to the annual quantity between 2009 and

2012 to 21% from 2015 to 2030. The second reduction step (to 63%) was enforced at the beginning of 2018. This has already led to a considerable price increase and shortage for some refrigerants (e.g., R134a). This regulation will make it necessary for manufacturers to retrofit, at least, some of their cycles to lower GWP refrigerants. Besides new plants, systems which are already in operation will perhaps have to be modified for further usage; the replacement of the working fluid is then the central point. Industry and academia started research on alternative refrigerants several years ago. Many criteria are important in the selection process of alternative refrigerants. Environmental aspects or material compatibility are important, but thermodynamic criteria are often crucial for the selection procedure. This is the focus of the present work. There are two main approaches in the search for alternative fluids. In the first approach, pure substances or fluid mixtures should have thermodynamic properties which are similar to the fluids to be substituted. The hydro-fluoro olefins (HFOs) such as R1234ze(E) or R1234yf, have come into focus [4] in this context. The advantage of this method is that the selection of a substitute is only based on the refrigerant used so far. These fluids are often expensive and investigations often show lower coefficients of performance (*COP*) compared to the currently used fluids (R1234ze(E) or R1234yf for R134a) [5,6]. In addition, this procedure blocks the possibility of identifying more efficient working fluids, having differing thermodynamic properties. In such systems, greenhouse gas emissions result from the release of refrigerant due to leakage. Also indirectly, the production of the electricity necessary for operation leads to emissions, if the electricity is mainly produced from fossil fuels. Although, the working fluid replacement with lower GWP fluids is useful, the *COP* should not be reduced and it would be better if improved. The second approach for fluid selection is based on the plant, and not on the fluid, which was used up to now. This seems to be more promising. Numerous publications were published in recent years which deal with such an approach and they often try to identify alternative fluids on a theoretical basis [7–10]. Such studies focus mostly on future plants and use very simple theoretical models where heat exchangers often are not modeled and compressor efficiencies are assumed to be fluid independent. For new plants, these kinds of studies are well justified because the fluid selection is part of the design process, as the selection of compressors and heat exchangers are. If instead a replacement fluid for a given existing system is needed then things change because e.g., it can no longer be assumed that the compressor will work equally well with any fluid. Similar approaches are seen in experimental studies which investigate the general suitability and efficiency of different fluids in a laboratory scale test-rig [6,11–13] or in single components like compressors or heat exchangers [14–16]. These investigations often lead to interesting heuristics, but they are not very helpful in finding replacement fluids for a concrete plant since the *COP*, heat flow rates and compressor power of another concrete system will have with a different fluid cannot be estimated. These are important criteria in determining whether a potential fluid is suitable at all or if other system components must be replaced. Modern process simulations seem to be most promising in finding individual replacement fluids, regarding the large number of plant designs. It remains unclear how detailed a concrete plant design must be modeled to obtain a reliable ranking of working fluids.

This uncertainty is addressed here. A vapor compression heat pump test-rig is simulated as a function of working fluid with thermodynamic models with three different complexity levels. The simulation results are compared along the different model depth levels and with measured values derived from a heat pump test-rig. Here, the fluids R134a, R152a, propane, propene, isobutane and dimethyl ether are investigated theoretically and experimentally at the same operating conditions as the heat pump. It is hypothetically assumed that R134a is the fluid to be substituted and thus the R134a results are always taken as a reference.

2. Experimental Investigation

The test-rig was a simple water/water vapor compression heat pump cycle as shown by a simplified scheme given in Figure 1. The main components were a semi-hermetic reciprocating compressor (GEA Bock: HG12P5.4; maximum power ($P_{\max} = 2.2$ kW)), an expansion valve, a condenser, and an evaporator.

Both heat exchangers were designed as counter flow double pipe heat exchangers and the expansion valve was a simple needle valve which allowed the experimenter to control the evaporation temperature independently from other process parameters. The system was equipped with extensive measuring technology. Pressure and temperature were measured at the in- and outlets of each component and a frequency converter recorded the electrical compressor power input. The secondary mass flow rates in the heat exchangers were also adjustable and were calibrated gravimetrically. The exact specifications of the system components and installed instrumentation can be found in Reference [11]. The recording and processing of the measured values were carried out in LabVIEW [17], while enthalpies, entropies and further thermodynamic properties were calculated with REFPROP [18]. Based on the given tolerances from the manufacturers of the used thermometers, pressure sensors, etc. the statistical errors were estimated based on a typical working point (propane, evaporator temperature ($T_{ev} = 0.0$ °C, condenser temperature ($T_c = 33.4$ °C, $n_{com} = 50$ Hz) by using error propagation. The maximum relative errors were $\pm 2.2\%$ for the COP , $\pm 0.3\%$ for the electrical compressor power, and $\pm 2.1\%$ for the rejected heat flow rate, however, reproduction measurements show errors below 2.0% for all these parameters. Statistical errors of other process variables are on the same order of magnitude.

2.1. Case Study and Boundary Conditions

The heat pump operating conditions were based on those of underfloor heating. Water, as a secondary fluid, entered the condenser at 25 °C (index: w, c, i) and the water mass flow rate was adjusted to a constant outlet temperature of 35 °C (index: w, c, o). The mass flow rate and temperature of the water entering the evaporator were both constant at $7.5 \text{ kg}\cdot\text{min}^{-1}$ and 17 °C, respectively. The water outlet temperature depended on the refrigerant and the evaporation temperature. The compressor rotation speed of 1500 min^{-1} was always fixed. The condenser water mass flow rate and the opening of the expansion valve, which was directly connected to the evaporation temperature, were the two experimental setting parameters of the heat pump. Within the experiments, these parameters were always adjusted to reach a maximum COP .

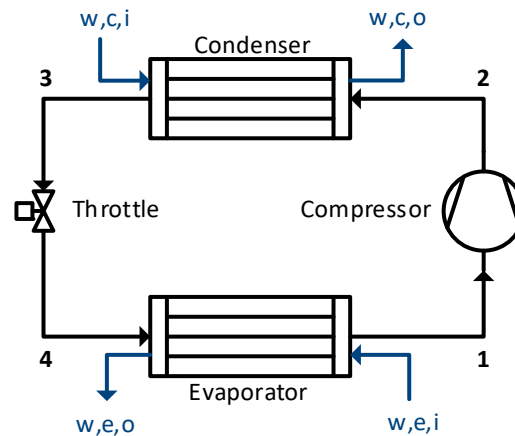
From a technical point of view, the operation of the test-rig is subject to some restrictions. Based on the partly flammable refrigerants, the minimum system pressure was restricted to 100 kPa in order to prevent the intake of ambient air into the system in the event of a leakage. With respect to mechanical stability, the maximum system pressure was set to 2 MPa. In addition, the refrigerant had to always be superheated by 3 K at the evaporator outlet in order to protect the compressor. Although the condenser water mass flow rate was one of the control parameters, it was limited to a maximum of $7.5 \text{ kg}\cdot\text{min}^{-1}$ due to the available infrastructure. The water temperature at the evaporator outlet had to always be above 2 °C to avoid freezing.

2.2. Experimental Results for R134a

The hypothetical case study considered in this work includes the assumption that the heat pump was previously operated with R134a which should now be substituted. Always, when a physical model of the respective simulation level cannot determine some necessary process parameters, it is assumed that the fluids perform similar to R134a. Due to the great importance of these values, they are discussed here, prior to the actual results. Table 1 summarizes the most important values. At the operating point with the highest efficiency the system with R134a had a COP of 4.76 and the rejected heat flow rate was $\dot{Q}_H = 3.85 \text{ kW}$. Due to pressure drops (Δp_i) in the heat exchangers, the evaporation and condensation temperatures were not constant. Here, the given evaporation temperature was the measured temperature at the evaporator inlet ($T_{ev} = 9.89$ °C) while the condensation temperature was the saturation temperature at the inlet pressure of the condenser ($T_c = 34.51$ °C). Furthermore, for R134a both superheating at the evaporator outlet and sub-cooling at the condenser outlet were observed. The smallest temperature differences between the secondary fluids and the refrigerant (pinch-temperatures) were 1.43 K inside the evaporator and 0.71 K inside the condenser, respectively.

Table 1. Measured data of the reference fluid R134a.

Parameter	Value	Parameter	Value
coefficient of performance, COP	4.76	pinch-temperature evaporator, $\Delta T_{Pinch,ev}$	1.43 K
rejected heat flow rate, \dot{Q}_H	3.85 kW	condensation temperature, T_c	34.51 °C
electrical compressor power, P_{com}	0.81 kW	sub-cooling condenser outlet, $\Delta T_{subcooling}$	2.11 K
evaporation temperature, T_{ev}	9.89 °C	pressure loss condenser, Δp_c	21.56 kPa
compressor inlet temperature, T_1	14.89 °C	pinch-temperature condenser, $\Delta T_{Pinch,c}$	0.71 K
pressure loss evaporator, Δp_{ev}	64.65 kPa	isentropic compressor efficiency, η_{com}^s	0.47

**Figure 1.** Heat pump scheme of the simulation models and the experiment.

3. Modeling

All simulation programs were written in the programming language Python [19] and the fluid properties were taken from the database REFPROP [18]. At simulation level II, a numerical optimizer non-linear problem (NLP) was used, taken from the OpenOpt network [20]. The simulations were based on the process scheme given in Figure 1 and the state numbers in the following were referenced to those given in Figure 1. For all simulation levels, an isenthalpic expansion in the throttle was assumed and the heat exchangers were considered to be adiabatic against the environment. The conditions and restrictions of the test-rig were set as described and applied similarly in all simulations.

3.1. Simulation Level I

Simulation level I included only a simple thermodynamic cycle calculation with specific values and largely ideal conditions. Constant isentropic compressor efficiencies were used for all fluids and heat exchanger pressure losses were neglected as is frequently used for fluid selection by other authors [7,8]. Since no physical models were implemented for the different components, numerous cycle states had to be specified. These included the evaporation temperature T_{ev} , the condensation temperature T_c , the compressor inlet temperature T_1 , the sub-cooling $\Delta T_{subcooling}$ at the condenser outlet, and the isentropic compressor efficiency η_{com}^s . Simulation level I did not capture the differences in operating conditions when different fluids were used in a concrete system. Here, the simplest and obvious assumption was that all components, such as heat exchangers and the compressor, operated similarly with different fluids. Thus, the required process variables were set here to the values which were measured with the reference fluid R134a (Table 1).

3.2. Simulation Level II

The second level was based on simulation level I but was significantly expanded by implementing a compressor model. The compressor model used was a semi-physical model which predicted volumetric and isentropic efficiencies as a function of the inlet state, the outlet pressure, and the working fluid. It was easily fitted to a concrete reciprocating compressor. It is already described in

detail in Reference [21] and will be summarized only briefly here. Apart from the state change of the gas in the cylinder, also friction of the piston, wall heat transfer, a clearance volume, and the valve flows were modeled. For the fluid dependent characterization of the valve flows empirical correlations were derived based on extensive measurement data for different fluids which determined the flow losses as a function of the fluid and the operation conditions. Finally, the model was based on four geometry parameters that either were known from the manufacturer or could be estimated in good approximation (bore, stroke length, outer surface, rod/crank length ratio) as well as only two further parameters (relative clearance volume c_{cl} and friction pressure p_{fr}) which had to be fitted to compressor dependent measured data. These fitting parameters can be estimated for a concrete compressor based only on the measurement of the volumetric and isentropic efficiencies at a single operating point with one fluid. A validation study with different fluids showed mean deviations of 3.0% for the isentropic efficiencies and 2.3% for the volumetric efficiencies while the maximum errors were still less than 6.0%. Besides the compressor used for model development, the model was also successfully applied to another reciprocating compressor. For the compressor used here the fitting led to a relative clearance volume of $c_{cl} = 0.61$ and a friction pressure of $p_{fr} = 48.92$ kPa.

The heat exchangers at this simulation level were modeled with pinch-models, which means for the respective heat exchangers that the lowest temperature difference over the entire length could not fall below a minimum value of $\Delta T_{pinch,i}$. These minimum values were directly related to the transfer capability or the quality of the heat exchangers but normally depended on the fluid and the flow conditions. However, the implemented models did not allow the exact estimation of the pinch-temperatures for different fluids and thus it was again assumed that the pinch-temperatures were equal to the measured values of the reference fluid R134a (Table 1). Despite the implemented pinch-models, there were no closed mathematical solutions for the heat exchangers. In the evaporator the outlet states of the water and of the refrigerant were unknown and in the condenser the unknown values were the outlet state of the refrigerant and the necessary water mass flow rate to reach a water heating from 25 °C to 35 °C. In each case, one of these process variables had to therefore be fixed to obtain a mathematical solution. The sub-cooling at the condenser outlet, as well as the outlet temperature of the evaporator (refrigerant), were selected analogous to level I. Again, it was assumed that the values corresponded to the measured values of R134a (Table 1). The values of the temperatures for evaporation and condensation, which were also still degrees of freedom of the simulation, were not taken from the reference fluid but were the values at the numerical maximum of the COP, analogous to the experiment. The optimization problem can be formulated as follows:

$$\begin{aligned} & \max_{T_{ev}, T_c} COP(T_{ev}, T_c) \\ & \vec{g}(T_{ev}, T_c) < 0 \\ & T_{ev, \min} \leq T_{ev} \leq T_{ev, \max} \in \mathbb{R}^{>0} \\ & T_{c, \min} \leq T_c \leq T_{c, \max} \in \mathbb{R}^{>0} \end{aligned} \quad (1)$$

The optimization parameters were box-bounded by meaningful parameter ranges ($T_{ev} = [-3 \text{ °C}, 17 \text{ °C}]$, $T_c = [25 \text{ °C}, T_{critical} - 5 \text{ K}]$) and the optimizations themselves were subjected to various constrains formulated as inequality constrains \vec{g} which referred to the described boundary conditions and restrictions of the test-rig as well as to the minimum pinch-temperatures (Table 1). All optimizations were repeated several times with different initial conditions in order to ensure a stable optimum. Also, the sensitivities of the optimized parameters in the region of the optima were analyzed; this increased the confidence in the optimizations and was also helpful for the discussion of the results.

3.3. Simulation Level III

In addition to the compressor model, at simulation level III a detailed model of the counterflow double-pipe heat exchangers was also included to calculate the heat transfer rates and the pressure

drops for the fluids. The heat-exchanger model was based on the cell method [22]. The heat transfer between the refrigerant and the secondary fluid took place along a series of two convective heat transfer steps and the heat conduction through the inner pipe wall. According to the different sections, where evaporation, condensation or superheating took place, different correlations for heat transfer and pressure drop were implemented, as given in Table 2. These correlations were, in a pre-selection study, found to be particularly suitable. The heat exchanger model indeed significantly expanded the entire model, but the evaporation and the condensation temperatures were still degrees of freedom of the simulation. The test-rig evaporation temperature was experimentally controlled by the expansion-valve orifice-opening, and thus, was a degree of freedom. But the resulting condensation temperature depended on the mass flow rate of the secondary fluid and on the interaction between the expansion valve and the compressor. The expansion valve used here was a simple needle valve, which is difficult to model, especially due to the two-phase flow. As a result, at simulation level III the evaporation and condensation temperatures were again taken as the values at the numerically maximal *COP*. These optimizations were subjected to the same boundary conditions as in level II or in the experiments. In case of a commercial plant equipped with an expansion device with a fixed control characteristic, this could also be implemented in the model and the optimization would no longer be necessary.

Table 2. Implemented correlations for heat transfer and pressure drop.

Model	Source
pipe flow ¹	Shah/Gnielinski VDI-Heat Atlas [22] (pp. 693–699)
concentric annular ¹	Martin/Stephan/Gnielinski VDI-Heat Atlas [22] (pp. 701–705)
pipe flow ² (evaporation)	Shah [23]
pipe flow ² (condensation)	Shah [24]
pressure drop ¹	VDI-Heat Atlas [22] (pp. 1057–1063)
pressure drop ²	VDI-Heat Atlas [22] (pp. 1125–1129)

¹ single phase flow, ² two phase flow.

4. Discussion and Results

Figure 2 shows the results of all fluids for the different simulation levels together with the experimental results. The x-axis is always divided into the different simulation levels (Sim-I–III) and the experiments (Exp.). The results of the presented parameter for one case (Sim-I–III, Exp.) therefore always lie on a vertical line. Figure 2 is divided into plots of the coefficient of performance (a), the rejected heat flow rate (b) and the compressor power input (c). For the experimental results, error bars are included that refer to the statistical errors as given in Section 2.2. Furthermore, Figure 3 shows a *T*–*s*-plot including the resulting thermodynamic cycles for all simulation levels and for the experiment exemplarily for the reference fluid R134a. All values of the discussed process parameters are summarized in the Supplementary Material (Tables S1 and S2). Here, all values used as input parameters of the respective simulation levels are indicated by italic letters.

First of all, from Figure 2 it is clear that the rejected heat flow rate and the compressor power input cannot be calculated by the simple calculations of simulation level I, though these are important parameters for the selection of replacement fluids. For example, if a potential replacement fluid would lead to a compressor power above the maximum power input of the used compressor either the fluid is generally not suitable, or the compressor has also to be replaced. From Figure 2a it is recognized that only small differences for the *COP*s between the fluids result from the level I calculations. For example, the maximum *COP* calculated in level I (isobutane) was just 1.04 times higher than the smallest calculated value (propene), whereas a ratio of 1.18 was observed from the measurements. This result is expected since the same evaporation and condensation temperatures as well as the same isentropic compressor efficiencies (taken from R134a) were considered for all fluids, although these values differ significantly, as observed in the measurements. For example, propane showed in the experiments a maximum evaporation temperature of 7.33 °C and an isentropic compressor efficiency

of 52%, whereas the values for R134a, which were also the basis for the calculation of propane, are 9.89 °C and 47% (Table 1). The isentropic compressor efficiency is of special importance since it differs significantly for different fluids (e.g., isobutane: 46%, propene: 64%) and also has a large influence on the COP of the entire process [11]. The marginal differences in the calculated COPs in the simulation level I were therefore only due to deviating fluid properties such as the evaporation enthalpy or the heat capacity ratio ($\kappa = c_p/c_v$). Actually, the only fluid for which physically meaningful values of the process parameters were considered in level I was the reference fluid R134a. However, the COPs resulting from level I ($COP = 5.35$) and from the experiment ($COP = 4.76$) differed greatly too. This was mainly due to neglecting pressure drops in the heat exchangers which is also illustrated in the T - s -plot (Figure 3). The pressure losses led primarily to a higher pressure ratio in the compressor and thus to a higher compressor power while the rejected heat flow rate remained nearly constant. Besides the absolute values of the COP, the relative comparison to the fluid to be replaced (reference fluid R134a) is also of great interest in the search for a direct substitution fluid since the information whether a fluid will have a higher or a lower COP than the one to be substituted is already helpful. However, the calculations of level I also led to a fluid order differing from the experimental order so they were not helpful for the selection of suitable substitution fluids.

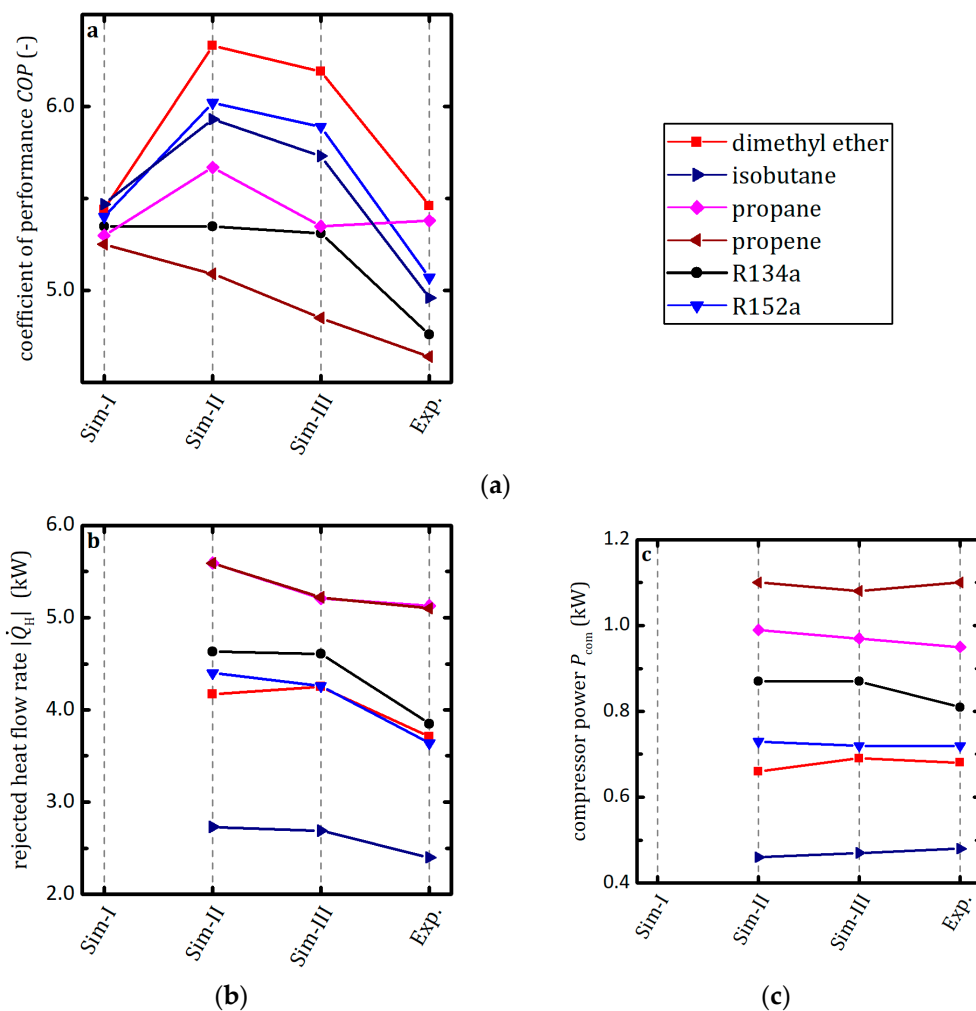


Figure 2. Coefficients of performance (a), rejected heat flow rates (b) and compressor power (c) for different fluids and for three simulation levels and the experiments.

The implementation of a compressor model and a pinch-model for the heat exchangers (simulation level II) also allows the model to estimate the expected heat flow rate and the compressor power.

Regarding the *COPs* in Figure 1, the results are now significantly improved, although a comparison with the measured values shows that the calculated *COPs* were, averaged over all fluids, about 14% too large. The situation is similar for the rejected heat flow rates; the calculated values were all too large. On the other hand, the values of compressor power were predicted with only small deviations ($\approx 3.5\%$). The deviations were again mainly due to the neglect of the pressure losses (Figure 3). Neglecting the pressure loss in the evaporator led to a too high pressure at the compressor inlet and thus to a decreased specific volume and to a smaller pressure ratio. The smaller pressure ratio caused a decreased specific compressor work while the decreased specific volume at the compressor inlet led to increased mass flow rates. Since the specific rejected heat remained nearly constant, the calculated heat flow rates were largely too high. Coincidentally, there were two counteracting effects in the compressor. The underestimated specific compressor work was counteracted by the overestimated mass flow rates so that overall the calculated values of the compressor power differed only slightly from the measurements. As a result, the calculations of level II led to overestimated *COPs*. The relative comparison to the fluid to be substituted showed that the simulation level II already led to adequate results. Based on the calculated values, it is possible to estimate with good accuracy whether a fluid will have higher or lower values of *COP*, rejected heat flow rate and compressor power, all in comparison to the previously used fluid. There are also some deviations. For example, it was predicted that propane has a smaller *COP* compared to isobutane and R152a, contradicting the experiments. In practice, a significant advantage of propane was observed. Nevertheless, level II is a helpful tool for a pre-selection step of suitable substitution fluids. If the resulting process of the fluid to be substituted is known from the considered plant it can reliably be estimated whether a fluid will at least reach the same rejected heat flow rate, whether it is compatible with the compressor installed, in terms of maximum power, and whether it will have a higher or a lower *COP*. The comparison with the results of level I showed that a good model for the calculation of the fluid dependent compressor efficiency is indispensable while already simple and unspecific models for the heat exchangers lead to reasonable results. An additional advantage of the simulation level II was the low computation time. The calculation of one fluid running on a standard computer (CPU: Intel Core i7-4790, RAM: 24 GB) only took a few minutes so that even large fluid databases could be searched for suitable fluids in a relatively short time.

In addition to the compressor model, the simulation level III also included detailed models for the calculation of heat transfer and pressure drop in the heat exchangers. This led in part to improved results with respect to level II and a better agreement with the experiments, as obvious from Figure 2. Compared to the results of level II, the *COPs* were calculated to be significantly smaller but they were still too high with respect to the measurements. The calculated order of fluids with respect to their *COPs* was not significantly improved and the wrong assessment regarding propane compared to isobutane and R134a remained. From the calculated rejected heat flow rates and compressor power it becomes clear that the overestimated *COPs* resulted primarily from overestimated heat flow rates since the calculated values of the compressor power fitted well to the measurements. In contrast to level II, the deviations here were not due to neglecting pressure drops. Rather, the optimization of the condensation temperatures was prone to error. In real cycles, the condensation temperature results from the interaction of all components. Due to a missing model for the expansion valve, however, this could not be simulated here. Alternatively, the condensation temperature was numerically optimized with respect to maximum *COP* as described previously. However, it can be observed from the data, and from the T - s -plot (Figure 3), that the numerical optimum was always located at unrealistically high condensation temperatures. The slightly overestimated condensation temperatures led to increased temperature differences between the refrigerant and the secondary fluid in the condenser (the temperature change of the secondary fluid was constant) and thus to higher heat flow rates. This also led to an increased sub-cooling at the condenser outlet (Figure 3). Overestimated heat flow rates at unchanged compressor power resulted in overestimated *COPs*. Because this effect was of numerical origin it could not be observed in the experiments. A solution would be either the

implementation of a good expansion valve model or a limitation of the maximum pinch-temperature within the optimization. Although the results were not significantly improved from level II to level III, the simulation level III had benefits. Level II already enabled the estimation of the expected heat flow rates but only the detailed heat exchanger models of level III made it possible to determine whether the heat exchangers were actually of sufficient size. In this context, the study also showed that accurate results can already be achieved with standard heat transfer correlations. Furthermore, in level III less information of the performance of the fluid to be replaced was necessary, so that also less measurement equipment was needed. However, a disadvantage of the further implementations of physical models at level III is the increasing computational time. The optimization of the process temperatures in level III currently takes up to a few hours per fluid on a standard computer. Although it is assumed that the required computational time can be significantly reduced in future, it will always be a multiple of the computational time of level II.

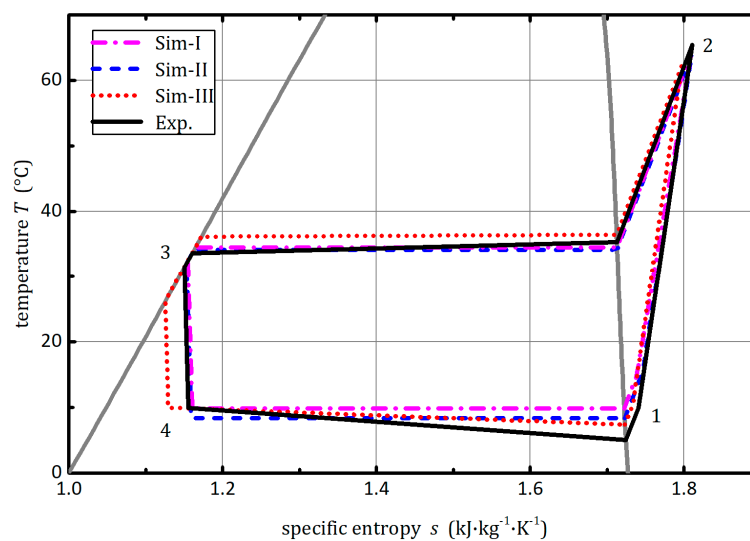


Figure 3. Temperature–entropy (T – s)-plot of the thermodynamic cycles resulting for R134a from the different simulation levels and the experiments.

5. Summary and Conclusions

In this work theoretical methods for identifying optimal replacement refrigerants for existing vapor compression refrigeration systems and heat pumps were investigated. The focus was on the so far unclear question of how detailed a concrete plant must be modeled in a simulation to achieve a reliable fluid ranking useful for fluid selection. To investigate this question a vapor compression heat pump test-rig was simulated by thermodynamic models with different levels of complexity. The results of the modeling were compared with measurements for different fluids, while R134a was defined as the refrigerant to be substituted. It turned out that simple cycle calculations with the assumption of constant process conditions and constant isentropic compressor efficiencies (level I) were not suitable for identifying potential substitution fluids for existing concrete plants. The implementation of a compressor model for a fluid-dependent and process-dependent determination of isentropic and volumetric efficiencies in combination with pinch-models for the heat exchangers (level II) significantly improved the results. Even though the absolute values partly differ from the measurements, the relative comparison to the fluid to be substituted showed good agreement with the measured values leading to a reliable estimation whether a fluid was more efficient than the fluid to be replaced and whether the rejected heat flow rate and the compressor power would be larger or smaller. The implementation of detailed models for the heat transfer and the pressure drop in the heat exchangers (level III) improved the results only slightly but the extensive models provided further information, e.g., whether the heat exchangers were of sufficient size to transfer the respective heat loads.

In summary, the study has shown that a good model for calculating compressor efficiencies is the minimum requirement for an effective search for replacement fluids for a specific plant. The compressor model used here can also be applied to other reciprocating compressors. For the model fitting only the four geometric parameters must be known as well as the isentropic and volumetric efficiencies for one operating point with one fluid. If different compressor types (screw, scroll etc.) are installed, the compressor model must be replaced accordingly. For the heat exchangers, it was shown that simple pinch-models are, at least for a preselection step, already a good approach which can easily be applied also to other types of heat exchangers (plate heat exchangers, crossflow etc.). However, this does not apply to the extensive model used here (level III) as it was developed only for double-pipe heat exchangers. Nevertheless, similar models can also be designed for other types of heat exchangers. In the future, software that includes models for different types of compressors and heat exchangers which can be individually combined with respect to the specific plant would be very helpful.

Due to the high computational effort of level III compared to level II, the high complexity model is not recommended to scan large refrigerant databases. Rather, it is recommended to carry out a preliminary study at level II and then to consider some of the identified fluids with a detailed model at level III. Although the simulations do not replace final experimental tests, they should be very helpful to select a reduced number of potential substitution fluids and reduce the number of required experiments.

Supplementary Materials: The following are available online at <http://www.mdpi.com/1996-1073/12/12/2417/s1>, Table S1: Data of dimethyl ether, isobutane and propane. Table S2: Data of propene, R134a and R152a. These tables provide the values of all discussed process parameters for all simulation levels and for the experiments. Italic letters indicate input values of the simulations and regular letters specify results.

Author Contributions: D.R. conceived the present idea and developed and carried out the simulations. V.V. planned and carried out the experiments. B.A. was the project administrator, supervised the project and was in charge of the overall direction. Result processing and interpretation was a joint process.

Funding: This research received no external funding.

Conflicts of Interest: The authors declare no conflicts of interest.

Nomenclature

I, II, III	simulation levels
c_{cl}	relative clearance volume (compressor model)
c_p	isobaric heat capacity, $J \cdot kg^{-1} \cdot K^{-1}$
c_v	isochoric heat capacity, $J \cdot kg^{-1} \cdot K^{-1}$
\vec{g}	vector of constraint functions
h	specific enthalpy, $J \cdot kg^{-1}$
\dot{m}	refrigerant mass flow rate, $kg \cdot s^{-1}$
P_{com}	electrical compressor power, W
p	pressure, Pa
p_{fr}	friction pressure (compressor model), Pa
\dot{Q}_H	rejected heat flow rate (condenser), W
q_H	specific rejected heat (condenser), $J \cdot kg^{-1}$
s	specific entropy, $J \cdot kg^{-1} \cdot K^{-1}$
T	temperature, K or $^{\circ}C$
w_{com}	specific compressor work, $J \cdot kg^{-1}$
Greek symbols	
Δi	difference of i
η_{com}^s	isentropic compressor efficiency
κ	heat capacity ratio

Subscripts and superscripts

1, 2, 3, 4	cycle states
c	condenser
com	compressor
ev	evaporator
i	inlet
max	maximum
min	minimum
o	outlet
w	secondary heat transfer fluid water

References

1. United Nations Environment Programme UNEP. Montreal Protocol on Substances that Deplete the Ozone Layer. 1987. Available online: www.unep.org (accessed on 21 June 2019).
2. European Union. *Verordnung über Fluorierte Treibhausgase*; EU: Brussels, Belgium, 2014; p. 517.
3. Intergovernmental Panel on Climate Change (IPCC). Working Group I Contribution to the IPCC Fifth Assessment Report: Climate Change 2013: The Physical Science Basis. Available online: http://www.climatechange2013.org/images/uploads/WGIAR5_WGI-12Doc2b_FinalDraft_Chapter08.pdf (accessed on 21 June 2019).
4. Honeywell Deutschland. Solstice Kältemittel: Roadmap. Available online: https://www.honeywell-refrigerants.com/europe/wp-content/uploads/2017/05/FPR-004-2017-10-DE_Refrigerants_Roadmap_LR.pdf (accessed on 21 June 2019).
5. Li, Z.; Liang, K.; Jiang, H. Experimental study of R1234yf as a drop-in replacement for R134a in an oil-free refrigeration system. *Appl. Therm. Eng.* **2019**, *153*, 646–654. [[CrossRef](#)]
6. Sánchez, D.; Cabello, R.; Llopis, R.; Arauzo, I.; Catalán-Gil, J.; Torrella, E. Energy performance evaluation of R1234yf, R1234ze(E), R600a, R290 and R152a as low-GWP R134a alternatives. *Int. J. Refrig.* **2017**, *74*, 269–282. [[CrossRef](#)]
7. Brown, J.S. Predicting performance of refrigerants using the Peng–Robinson Equation of State. *Int. J. Refrig.* **2007**, *30*, 1319–1328. [[CrossRef](#)]
8. Dalkilic, A.S.; Wongwises, S. A performance comparison of vapour-compression refrigeration system using various alternative refrigerants. *Int. Commun. Heat Mass Transf.* **2010**, *37*, 1340–1349. [[CrossRef](#)]
9. Saleh, B.; Wendland, M. Screening of pure fluids as alternative refrigerants. *Int. J. Refrig.* **2006**, *29*, 260–269. [[CrossRef](#)]
10. Roskosch, D.; Atakan, B. Reverse engineering of fluid selection for thermodynamic cycles with cubic equations of state, using a compression heat pump as example. *Energy* **2015**, *81*, 202–212. [[CrossRef](#)]
11. Venzik, V.; Roskosch, D.; Atakan, B. Propene/isobutane mixtures in heat pumps: An experimental investigation. *Int. J. Refrig.* **2017**, *76*, 84–96. [[CrossRef](#)]
12. Fang, Y.; Croquer, S.; Poncet, S.; Aidoun, Z.; Bartosiewicz, Y. Drop-in replacement in a R134 ejector refrigeration cycle by HFO refrigerants. *Int. J. Refrig.* **2017**, *77*, 87–98. [[CrossRef](#)]
13. Cabello, R.; Sánchez, D.; Llopis, R.; Arauzo, I.; Torrella, E. Experimental comparison between R152a and R134a working in a refrigeration facility equipped with a hermetic compressor. *Int. J. Refrig.* **2015**, *60*, 92–105. [[CrossRef](#)]
14. Chang, Y.; Kim, M.; Ro, S. Performance and heat transfer characteristics of hydrocarbon refrigerants in a heat pump system. *Int. J. Refrig.* **2000**, *23*, 232–242. [[CrossRef](#)]
15. Mendoza-Miranda, J.M.; Mota-Babiloni, A.; Ramírez-Minguela, J.J.; Muñoz-Carpio, V.D.; Carrera-Rodríguez, M.; Navarro-Esbri, J.; Salazar-Hernández, C. Comparative evaluation of R1234yf, R1234ze(E) and R450A as alternatives to R134a in a variable speed reciprocating compressor. *Energy* **2016**, *114*, 753–766. [[CrossRef](#)]
16. Miyara, A. Condensation of hydrocarbons—A review. *Int. J. Refrig.* **2008**, *31*, 621–632. [[CrossRef](#)]
17. National Instruments. *LabVIEW Professional Development System*; National Instruments: Austin, TX, USA, 2013.
18. Lemmon, E.W.; Huber, M.L.; McLinden, M.O. *NIST Standard Reference Database 23*; National Institute of Standards and Technology: Gaithersburg, MD, USA, 2013.
19. Python.org. Available online: <https://www.python.org/> (accessed on 21 June 2019).

20. OpenOpt. Available online: <http://openopt.blogspot.de/> (accessed on 21 June 2019).
21. Roskosch, D.; Venzik, V.; Atakan, B. Thermodynamic model for reciprocating compressors with the focus on fluid dependent efficiencies. *Int. J. Refrig.* **2017**, *84*, 104–116. [[CrossRef](#)]
22. Ingenieure, V.D. *VDI Heat Atlas*, 2nd ed.; Springer: Berlin, Germany, 2010; ISBN 978-3-540-77877-6.
23. Shah, M.M. A New Correlation for Heat Transfer During Boiling Flow Through Pipes. *Ashrae Trans.* **1976**, 66–86.
24. Shah, M.M. A general correlation for heat transfer during film condensation inside pipes. *Int. J. Heat Mass Transf.* **1979**, *22*, 547–556. [[CrossRef](#)]



© 2019 by the authors. Licensee MDPI, Basel, Switzerland. This article is an open access article distributed under the terms and conditions of the Creative Commons Attribution (CC BY) license (<http://creativecommons.org/licenses/by/4.0/>).

Fluid Retrofit for Existing Vapor Compression Refrigeration Systems and Heat Pumps

Roskosch, Dennis; Venzik, Valerius; Atakan, Burak

This text is provided by DuEPublico, the central repository of the University Duisburg-Essen.

This version of the e-publication may differ from a potential published print or online version.

DOI: <https://doi.org/10.3390/en12122417>

URN: <urn:nbn:de:hbz:464-20190814-115233-9>

Link: <https://duepublico.uni-duisburg-essen.de:443/servlets/DocumentServlet?id=49175>

License:



This work may be used under a [Creative Commons Attribution 4.0 International](https://creativecommons.org/licenses/by/4.0/) license.

Source: Energies 2019, 12, 2417; Published: 24 June 2019